J. Phys. Chem. A **2000,** *104,* 5111−5114

Existence of Posner's Cluster in Vacuum

Gabin Treboux,* Pierre Layrolle, Noriko Kanzaki, Kazuo Onuma, and Atsuo Ito

National Institute for Advanced Interdisciplinary Research, 1-1-4 Higashi, Tsukuba-shi, Ibaraki 305, Japan

Received: December 14, 1999; In Final Form: March 13, 2000

Using ab initio methods, a single isomer of D_{3h} symmetry was found to be preeminent on the $Ca_3(PO_4)_2$ cluster potential energy surface. This isomer has the distinct feature that each calcium atom is surrounded by four oxygen atoms. We studied the aggregation of this isomer in the $[Ca_3(PO_4)_2]_n$ system with n being 2 or 3. This gives us an energy reference for analyzing the stability of the so-called Posner's cluster $Ca_9(PO_4)_6$ which is the core of the actual structural model of amorphous calcium phosphate. Posner's cluster is shown to be significantly stabilized in comparison to the energy reference.

Introduction

Calcium phosphate clustering with a Ca/P molar ratio of 1.5 is extremely important from the viewpoint of vertebrate biomineralization because clustering is involved in the formation process of hydroxyapatite ($Ca_{10}(PO_4)_6(OH)_2$; HAP) which has a chemical and structural resemblance to bone and tooth minerals (see Figure 1).[1−3] Amorphous calcium phosphate (ACP) has been shown to form with a Ca/P molar ratio of 1.45 ± 0.05 as a precursor in the crystal growth process of HAP in vitro in a solution supersaturated as highly as a physiological solution.[4] ACP has also been implicated in the early stages of bone mineralization in vivo, and has been detected in young bones, intracellular deposits, and matrix vesicles,[5] although there are some controversial reports.[6] A structural model of ACP consists of elementary $Ca_9(PO_4)_6$ clusters, in which the Ca and PO_4 atomic positions are approximately the same as those in HAP.[2] We will refer to this structural model as Posner's cluster. Recently, in an aqueous solution, the presence of calcium phosphate clusters with dimensions similar to those of Posner's cluster has been demonstrated by a dynamic light scattering technique.[7] As a result, a cluster growth model in which HAP grows by hexagonal packing of Posner's clusters has been proposed.[7] Because the structural model of ACP or Posner's cluster was proposed solely on the basis of X-ray radial distribution analyses[2] that might permit a variety of interpretations, there may exist other possible structural models. Despite the importance of the cluster in the biomineralization process, no analysis through calculation has been reported to date. We have therefore investigated, through ab initio methods, the stability of calcium phosphate clusters. Few calculations have been reported for such systems.[8] The main difficulty is the number of different electronic situations obtained by varying the number of calcium atoms, PO_4 groups, or hydrogen atoms in the formula $Ca_xH_y(PO_4)_z$. In the present study, we focused on clusters having a Ca/P ratio of 1.5 because of the frequent appearance of this ratio in the experimental analyses. Interestingly, this is the only ratio attainable when positive Ca^{2+} and negative PO_4^{3-} ions are balanced without adding hydrogen atoms. This forms a family of neutral $[Ca_3(PO_4)_2]_n$ clusters. From a chemical point of view, this neutrality is a stabilizing factor. We have verified that the ground state of the clusters corresponds to a closed shell configuration. The wave function of each cluster can be calculated using the same restricted Hartree−Fock scheme and the calculated energies can be directly compared throughout the family of $[Ca_3(PO_4)_2]_n$ clusters in terms of $Ca_3(PO_4)_2$ monomer energy. In this study, all calculations were performed using a split valence plus polarization (SVP) basis set quality.[9,10]

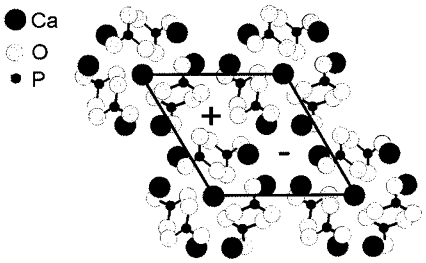

Figure 1. Schematic representation of the hydroxyapatite ($Ca_{10}(PO_4)_6(OH)_2$) crystal projected onto the ab crystallographic plane. Along the *c*-axis perpendicular to the view plane, the crystal organizes in columns composed of Posner's cluster $Ca_9(PO_4)_6$. The remaining atoms, two OH groups and one Ca atom per unit cell are incorporated in the voids among the clusters and form positive and negative columns parallel to the *c*-axis. The surface of the unit cell is delimited by black lines. Note that the aggregation of three Posner's clusters of identical chirality around the positive column leads to the formation of a supplemental Posner's cluster of opposite chirality.

Results and Discussion

(1) The Monomer Cluster $Ca_3(PO_4)_2$. A systematic search for the potential energy surface (PES) corresponding to the singlet state configuration was performed for the monomer $Ca_3(PO_4)_2$. Although there is no mathematical criterion to ensure that the global minimum has been found on the PES, we enumerated all the topologies possible with the restriction that the two PO_4 groups in which each phosphorus atom is surrounded by four oxygen atoms are conserved. We subsequently optimized the geometry of all these structures. This study has been reported in detail elsewhere.[11] The findings are summarized in Figure 2. An isomer of symmetry D_{3h} is preeminent in energy. The energy separation between this lowest energy minimum isomer and the closest local minimum is 82 kcal/mol. This isomer has the distinct feature that each calcium atom is surrounded by four oxygen atoms from PO_4 groups.

---

* Corresponding author: gabin@nair.go.jp.

10.1021/jp994399t CCC: $19.00

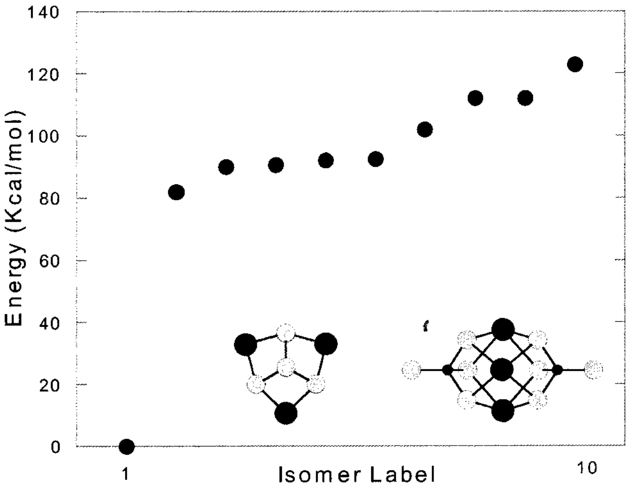

Figure 2. Energy of the different isomers on the $Ca_3(PO_4)_2$ PES. The 10 local minima associated with the lowest energies are considered. The insert shows the top and side views of the isomer of D_{3h} symmetry associated with the lowest energy minimum labeled 1.

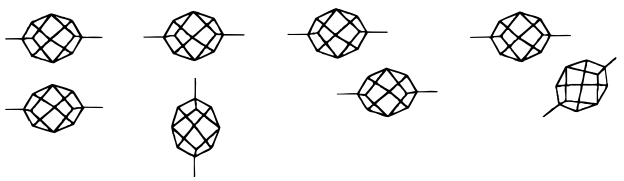

Figure 3. Four possible relative orientations of two separated $Ca_3(PO_4)_2$ monomers. For each relative orientation, three different geometries were defined by rotating one monomer around its C_3 axis by 0, 30, and 60 degrees. Each optimization of geometry was started from the two separated $Ca_3(PO_4)_2$ monomers taken in the geometry associated with the lowest energy minimum of the $Ca_3(PO_4)_2$ PES.

The geometries and energies obtained using the SVP basis set quality have been shown to be in good agreement with those obtained using the extended basis set quality.[11]

(2) The Aggregated Clusters $[Ca_3(PO_4)_2]_n$. Considering the presence of a single energy-preeminent isomer on the $Ca_3(PO_4)_2$ PES, we considered the aggregation of *n* such isomers to form $[Ca_3(PO_4)_2]_n$ clusters. First, the aggregation of two isomers was investigated by extending the system to $[Ca_3(PO_4)_2]_2$. It should be noted that the aggregate does not neccessarily correspond to the lowest energy minimum of the $[Ca_3(PO_4)_2]_2$ PES. However, the aggregate corresponds to the lowest energy minimum within those attainable, starting from two separated monomers, without overcoming an energy barrier. We have ensured that no energy barriers were overcome during the procedure to optimize geometry by ensuring that each step of the procedure corresponded to an energy lowering. The possible relative orientations of the two $Ca_3(PO_4)_2$ units taken into account are represented in Figure 3. After the geometry optimization, all calculations converged to a unique structure (see Figure 4). Once we obtained the geometry of the dimer, we added a third monomer to it and, without overcoming an energy barrier, similarly obtained the optimized geometry of the trimer. This gives us an energy reference to compare any cluster $[Ca_3(PO_4)_2]_n$ with *n* being 2 or 3.

(3) Posner's Cluster $Ca_9(PO_4)_6$. Posner's cluster in the HAP crystal appears with a higher symmetry than that of the trimer calculated in Section 2. Posner's cluster has a C_3 symmetry and two chiral forms in the HAP structure (see Figure 1). Starting from the atomic positions found in the HAP structure, the geometry optimization of the cluster performed within the C_3 group leads to an S_6 isomer (see Figure 5). This change in symmetry during the calculation was permitted because the C_3 group is a subgroup of the S_6 group. The calculation shows that Posner's cluster can reach this S_6 isomer without being trapped by a higher energy minimum. Considering a starting geometry of symmetry C_i, which is the second subgroup of the S_6 symmetry group, leads to an identical result, i.e., convergence to the S_6 isomer. These calculations show that the chirality feature of Posner's cluster disappears in a vacuum environment as the two chiral forms converge to the same centrosymmetric isomer.

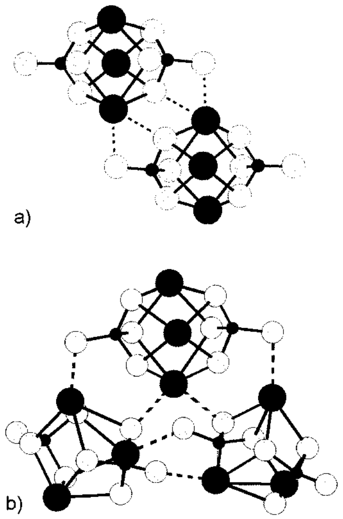

Figure 4. (a) Side view of the dimer formed by aggregation of two $Ca_3(PO_4)_2$ clusters. (b) Side view of the trimer formed by aggregation of three $Ca_3(PO_4)_2$ clusters. In these aggregated structures, four (dimer case) or six (trimer case) supplemental CaO bonds were created as represented by the dashed lines.

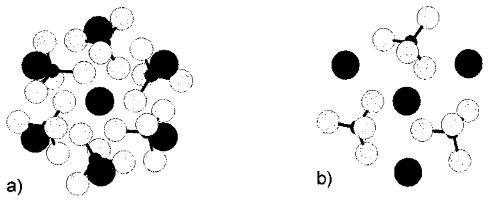

Figure 5. Top view of the isomer of S_6 symmetry. Three calcium atoms coincide with the C_3 axis. (a) complete cluster (b) top half of the cluster.

We now consider the geometrical distortions which do not necessarily conserve the C_3 axis. The systematic study of the PES associated with a system of such complexity as $Ca_9(PO_4)_6$ is most definitely not possible, even with state-of-the-art computer platforms. This PES contains a huge number of local minima which are structurally very different from Posner's cluster. Nonetheless, a study of the compact structures of the $Ca_9(PO_4)_6$ cluster, i.e., the structures in which the Ca and PO_4 parts are disposed closely together, is feasible. The compactness of the structures permits the creation of a large number of CaO interactions within the cluster. This appears to be the determining factor in the stability of the $Ca_3(PO_4)_2$ cluster. The most compact structures are obtained by placing one calcium atom at the center and at each corner of a cube, i.e., by forming an O_h arrangement, and by inserting the PO_4 groups among them to form CaO bonds. Considering the longest diagonals of the cube as C_3 axes, two structures of D_{3d} symmetry can be constructed. They differ in terms of their orientation of PO_4 groups (see Figure 6). Describing the orientation of each PO_4 group by an angle α, having the value 0 or 180 degrees, the structure of Figure 6a corresponds to the vector (0,0,0,0,0,0) while the structure of Figure 6b corresponds to the vector (180,180,180,180,180,180).

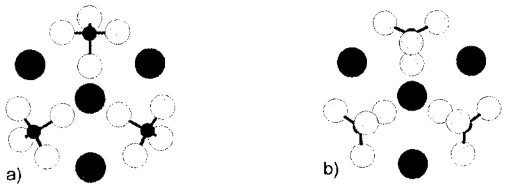

Figure 6. Top view of the two isomers of D_{3d} symmetry. Three calcium atoms coincide with the C_3 axis. Here, we show only the top halves of the clusters. The position of the atoms forming the lower halves are obtained through the application of a S_6 operation of symmetry. The isomers (a) and (b) differ in terms of their orientation of PO_4 groups. For each PO_4 group, there exists a rotational axis which permits a pass from orientation (a) to orientation (b) by a rotation of 180 degrees.

On the other hand, positioning one PO_4 group at each face of the cube permits the construction of structures of T_d or T_h symmetry. We describe here the orientation of each PO_4 group by the dihedral angle β between one σ_v plane of the PO_4 tetrahedron and one diagonal of the associated face of the cube. The T_d and T_h structures correspond to the vectors (0,0,0,0,0,0) and (45,45,45,45,45,45), respectively.

From these highly symmetric structures we considered all the situations obtained by rotating each PO_4 group independently. Considering the values of −45, 0, 45, and 90 degrees for the angle β and the T_h and T_d structures as starting points, exactly 123 different situations can be generated. Considering only the situations that have at least two operations of symmetry, we obtained a set of 57 structures ($1T_h$, $1T_d$, $5D_{2d}$, $3D_{2h}$, $4D_2$, $3C_{2v}$, $2C_{2h}$, $1S_4$, $2C_3$, $1C_i$, $21C_2$, $13C_s$). Identically, considering the values of 0 and 180 degrees for the angle α and the D_{3d} structures as starting points, 14 different situations can be generated. Considering only the situations that have at least two operations of symmetry, we obtained a set of 10 structures ($2D_{3d}$, $1C_{3v}$, $3C_{2h}$, $4C_s$). We subsequently optimized the geometry of these 67 structures. The point group symmetry associated with each structure was taken into account explicitly during the geometry optimization. The optimization of a structure of C_2 symmetry required, on average, one month of calculation time on an IBM workstation. On some occasions the structure did not correspond to any stationary point on the associated PES and therefore, some isomers were obtained several times from different starting geometries. For instance, the four initial geometries of D_2 symmetry converged to a single isomer. It should be noted that this set contains structures of C_3 and C_i symmetry which have not been considered when analyzing the C_3 symmetry. All these structures converged to the S_6 isomer.

The energies of all the stationary points of the PES found through this procedure are presented in Figure 7. The isomers are labeled by decreasing values of their number of symmetry operations in their point group symmetry. For example, the labels 1, 2, 3, and 4 correspond to isomers of T_d, T_h, D_{3d}, and D_{3d} symmetry, respectively. Calculated bond lengths have been compared with available experimental data in ref 12.

Due to the finite size of the clusters, the chemical environment of the Ca atoms is changed while transferring the cluster from the HAP crystal to a vacuum environment. Because each calcium atom has fewer neighboring oxygen atoms, distortions occur to optimize the CaO interactions. Therefore, as a general tendency, the energy of clusters decreases with a reduction in symmetry. However, the S_6 and T_h isomers have exceptionally low energies considering their high symmetries.

The isomers corresponding to the first, second, and third lowest energy calculated are of C_s, S_6, and C_2 symmetry, respectively. The associated energies are 0.0, 3.1, and 4.3 kcal/mol, respectively. Reoptimizing these structures using a B3LYP functional[10] led to similar results, i.e., 0.0, 3.9, and 4.9 kcal/mol, respectively. Taking into account the basis set superposition error effect and the fact that the calculations were performed using medium-quality basis sets, such energy differences have to be considered as indications only.

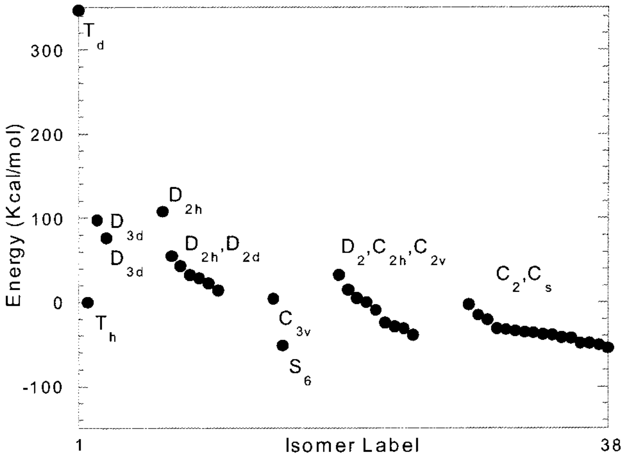

Figure 7. Energy of 38 stationary points found on the $Ca_9(PO_4)_6$ PES starting from a set of 67 highly symmetric structures. The stationary points are ordered by decreasing values of their number of symmetry operations.

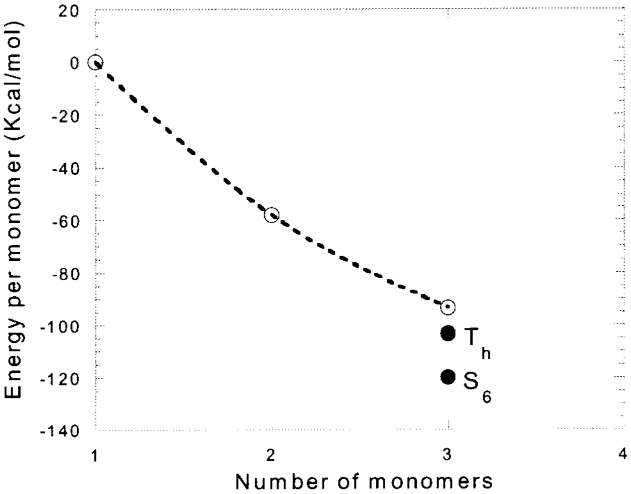

Figure 8. Stabilization energy per monomer $Ca_3(PO_4)_2$ as a function of the number of monomers in the $[Ca_3(PO_4)_2]_n$ cluster. The dashed curve links the stabilization energy calculated for the isolated monomer, the dimer obtained by aggregation of two monomers and the trimer obtained by aggregation of three monomers. The shaded circles represent the stabilization energy per monomer of the S_6 and T_h Posner's clusters in vacuum.

Next, we compare the energy of the $Ca_9(PO_4)_6$ isomers with the energy reference constructed in Section 2 (see Figure 8). The low-energy compact forms of the $Ca_9(PO_4)_6$ cluster are more stable than the corresponding trimer aggregate. This energy comparison is based on the energy expressed per monomer unit. The energy differences obtained are large in comparison with the error bar expected from the calculation method used. Considering only energy criteria, calcium phosphate materials with a Ca/P ratio of 1.5 are not likely to be present in ACP in a $Ca_3(PO_4)_2$ monomer form. However, a highly stable dimer structure could exist for the calcium phosphate material. The existence of such an energy preeminent structure for the dimer case is unlikely due to the following four points. (1) The monomer selected as a reference is preeminent in energy, being 82 kcal/mol more stable than the second lowest energy minimum on the $Ca_3(PO_4)_2$ PES. (2) The aggregation of two such monomers results in a huge supplemental stabilization energy of 58 kcal per monomer in the aggregated form. This arises from the formation of four supplemental CaO bonds in the aggregated structure. (3) The low-energy structures of Posner's cluster are considerably more stable than the dimer aggregate. The S_6 isomer, for instance, is 62 kcal per monomer more stable than the dimer aggregate. (4) We are currently performing a systematic search for the dimer case in continuation of the work we have carried out for the monomer PES,[11] starting the search from the most compact structures, and have not yet found any structures lower in energy than the dimer aggregate. The present results are consistent with the actual structural model of ACP which suggests that a significant amount of calcium phosphate material is present in ACP in the form of Posner's clusters.

Nonetheless, the result of the search on the PES shows undoubtedly that numerous isomers coexist within an energy range of a few kcal/mol. Note that supplemental isomers of symmetry C_1 might also exist within the same energy range. The assignment of ACP structure based on X-ray radial distribution function analyses should integrate this result because several different geometries might explain the experimental data.

Conclusions

Using ab initio methods, a single isomer with D_{3h} symmetry was found to be preeminent on the PES associated with the $Ca_3(PO_4)_2$ cluster. We studied the aggregation of this isomer in the systems $[Ca_3(PO_4)_2]_n$with n being 2 or 3. For the $[Ca_3(PO_4)_2]_3$ trimer case we found that an isomer of S_6 symmetry obtained from the geometry optimization of the so-called Posner's cluster was strongly stabilized in comparison with the trimer formed by aggregating three $Ca_3(PO_4)_2$ clusters. Several other isomers of lower symmetry, associated with similar energy, were also found. The calculations are consistent with the actual structural model of ACP. Nonetheless, further validation of this structural model through ab initio calculations is required to take into account the presence of water molecules around the clusters in the ACP. As mentioned by an anonymous referee, the balance between energy and entropy terms, which is not a preponderant effect for small clusters in a vacuum environment, should be of crucial importance in an aqueous solution environment. We are currently investigating the feasibility of this computational challenge.

Acknowledgment. The calculations were performed at the AIST Tsukuba Advanced Computing Center.

Supporting Information Available: HF and B3LYP optimized coordinates of the clusters.

References and Notes

(1) Kay, M. I.; Young, R. A.; Posner, A. S. *Nature* **1964**, *204*, 1050.

(2) Posner, A. S.; Betts, F. *Acc. Chem. Res.* **1975**, *8*, 273.

(3) Kim, H.; Rey, C.; Glimcher, M. J. *Calcif. Tissue. Int.* **1996**, *59*, 58.

(4) Nancollas, G. H.; Mohan, M. S. *Archs. Oral Biol.* **1970**, *15*, 731.

(5) Termine, J. D.; Posner, A. S. *Science* **1966**, *133*, 1523.

(6) Grynpas, M. D.; Bonar, L. C.; Glimcher, M. J. *Calcif. Tissue Int.* **1984**, *36*, 291.

(7) Onuma, K.; Ito, A. *Chem. Mater.* **1998**, *10*, 3346.

(8) Peeters, A.; De Mayer, E. A. P.; Van Alsenoy, C.; Verbeeck, R. M. H. *J. Phys. Chem. B* **1997**, *101*, 3995.

(9) Schafer, A.; Horn, H.; Ahlrichs, R. *J. Chem. Phys.* **1992**, *97*, 2571.

(10) Gaussian 98 (Revision A.7), M. J. Frisch, G. W. Trucks, H. B. Schlegel, G. E. Scuseria, M. A. Robb, J. R. Cheeseman, V. G. Zakrzewski, J. A. Montgomery, R. E. Stratmann, J. C. Burant, S. Dapprich, J. M. Millam, A. D. Daniels, K. N. Kudin, M. C. Strain, O. Farkas, J. Tomasi, V. Barone, M. Cossi, R. Cammi, B. Mennucci, C. Pomelli, C. Adamo, S. Clifford, J. Ochterski, G. A. Petersson, P. Y. Ayala, Q. Cui, K. Morokuma, D. K. Malick, A. D. Rabuck, K. Raghavachari, J. B. Foresman, J. Cioslowski, J. V. Ortiz, B. B. Stefanov, G. Liu, A. Liashenko, P. Piskorz, I. Komaromi, R. Gomperts, R. L. Martin, D. J. Fox, T. Keith, M. A. Al-Laham, C. Y. Peng, A. Nanayakkara, C. Gonzalez, M. Challacombe, P. M. W. Gill, B. G. Johnson, W. Chen, M. W. Wong, J. L. Andres, M. Head-Gordon, E. S. Replogle, J. A. Pople, Gaussian, Inc.: Pittsburgh, PA, 1998.

(11) Treboux, G.; Kanzaki, N.; Onuma, K.; Ito, A. *J. Phys. Chem. A.* **1999**, 103, 8118.

(12) Kanzaki, N.; Onuma, K.; Treboux, G.; Tsutsumi, S.; Ito, A. *J. Phys. Chem. B* **2000**, in press.